


p53 induction and cell viability modulation by genotoxic individual chemicals and mixtures

Carolina Di Paolo¹  · Yvonne Müller¹ · Beat Thalmann¹ · Henner Hollert^{1,2,3,4} · Thomas-Benjamin Seiler¹

Received: 10 September 2016 / Accepted: 8 March 2017 / Published online: 16 March 2017
© Springer-Verlag Berlin Heidelberg 2017

Abstract The binding of the p53 tumor suppression protein to DNA response elements after genotoxic stress can be quantified by cell-based reporter gene assays as a DNA damage endpoint. Currently, bioassay evaluation of environmental samples requires further knowledge on p53 induction by chemical mixtures and on cytotoxicity interference with p53 induction analysis for proper interpretation of results. We investigated the effects of genotoxic pharmaceuticals (actinomycin D, cyclophosphamide) and nitroaromatic compounds (4-nitroquinoline 1-oxide, 3-nitrobenzanthrone) on p53 induction and cell viability using a reporter gene and a colorimetric assay, respectively. Individual exposures were conducted in the absence or presence of metabolic activation system, while binary and tertiary mixtures were tested in its absence only. Cell viability reduction tended to present direct correlation with p53 induction, and induction peaks occurred mainly at chemical concentrations causing cell viability below 80%. Mixtures presented in general good agreement between

predicted and measured p53 induction factors at lower concentrations, while higher chemical concentrations gave lower values than expected. Cytotoxicity evaluation supported the selection of concentration ranges for the p53 assay and the interpretation of its results. The often used 80% viability threshold as a basis to select the maximum test concentration for cell-based assays was not adequate for p53 induction assessment. Instead, concentrations causing up to 50% cell viability reduction should be evaluated in order to identify the lowest observed effect concentration and peak values following meaningful p53 induction.

Keywords p53 tumor suppression protein · p53 pathway · DNA damage · Genotoxicity · Cytotoxicity · Reporter gene cell line bioassay

Introduction

Activation of the p53 tumor suppression protein has a central role in transcriptional regulation of a network of genes in response to stressors that interfere with DNA integrity and cell proliferation. Under undisturbed conditions, the p53 tumor suppressor protein is maintained at low levels by negative feedback loops, such as by the well-studied mouse double minute 2 (MDM2) homolog protein (Lavin and Gueven 2006; Beckerman and Prives 2010). However, a variety of DNA-damaging agents can interfere with this equilibrium, triggering p53 activation and stabilization and leading to its accumulation (Harris and Levine 2005; Kumari et al. 2014). The binding of p53 to DNA response elements (p53RE) will then result in transcriptional modulation of target genes and activation of the p53 regulatory network (Beckerman and Prives 2010). Several responses can follow, including DNA damage, cell cycle arrest, or apoptosis, ultimately promoting

Carolina Di Paolo and Yvonne Müller contributed equally to this work.

Responsible editor: Philippe Garrigues

✉ Carolina Di Paolo
carolina.dipaolo@bio5.rwth-aachen.de

- ¹ Department of Ecosystem Analysis, Institute for Environmental Research, Aachen Biology and Biotechnology (ABBt), RWTH Aachen University, Aachen, Germany
- ² College of Resources and Environmental Science, Chongqing University, 1 Tiansheng Road, Beibei, Chongqing 400715, China
- ³ College of Environmental Science and Engineering and State Key Laboratory of Pollution Control and Resource Reuse, Tongji University, 1239 Siping Road, Shanghai, China
- ⁴ State Key Laboratory of Pollution Control and Resource Reuse, School of the Environment, Nanjing University, Nanjing, China

tumor-protecting mechanisms (Harris and Levine 2005; Lavin and Gueven 2006; Beckerman and Prives 2010; Kumari et al. 2014).

Different *in vitro* bioassays have evaluated the activation of the p53 pathway as an endpoint for DNA damage in human health assessment. Levels of p53 protein can be measured by indirect immunofluorescence flow cytometry, ELISA, or Western blot analysis (Salazar et al. 1997; Yang and Duerksen-Hughes 1998; Clewell et al. 2014). Also, the activation of p53RE by p53 protein binding can be quantified through high-throughput assays with p53RE luciferase (p53RE-Luc) or p53RE β -lactamase reporter gene cell lines (Sohn et al. 2002; Kester et al. 2003; Briat and Vassaux 2008; Knight et al. 2009; van der Linden et al. 2014). Since p53 isoforms are active in non-mammal vertebrates (e.g., fish, amphibians) and invertebrates (e.g., clams, nematodes), the p53 pathway has also relevance for environmental risk assessment (Bhaskaran et al. 1999; Bensaad et al. 2001; Rutkowski et al. 2010; Storer and Zon 2010; Wernersson et al. 2015).

Still, knowledge gaps can hamper the application of such assays to evaluate environmental samples containing different contaminants. Limited information is available on p53 induction following exposure to chemical mixtures, since most of investigations have focused on individual compound exposure (Duerksen-Hughes et al. 1999; Knight et al. 2009; Salazar et al. 2009; van der Linden et al. 2014). Although p53 modulation after co-treatment with different drugs has been investigated by some studies, their focus was mainly of therapeutic concern (Choong et al. 2009; Chen et al. 2014; Zajkowiec et al. 2015). Also, the interference of cytotoxicity has been discussed to be an issue for p53 induction analysis in samples of water and animal tissue (Yeh et al. 2014; Jin et al. 2015), which can be related to the fact that high levels of p53 sensitize cells to DNA damage and can lead to decreased cell viability (Lutzker et al. 2001). Consequently, for the integration of p53 induction as an endpoint in the analysis of environmental samples, further knowledge is required on the correlation with cell viability and on the effects of mixtures.

In this study, we investigated the correlation between cell viability modulation and the induction of the p53 pathway using a p53RE-Luc cell line assay (van der Linden et al. 2014) following the exposure to genotoxic chemicals as individual exposure or mixtures. Tested compounds included the DNA-interacting drug actinomycin D (ActD) and the DNA-damaging prodrug cyclophosphamide (CPP) as model p53 inducers in the absence and presence of metabolic activation, respectively (Strauss et al. 2007; Choong et al. 2009). We also tested two nitroaromatic compounds, i.e., 4-nitroquinoline 1-oxide (NQO), a quinolone derivative and UV-mimetic DNA-damaging chemical (Han et al. 2007), and the diesel exhaust component 3-nitrobenzanthrone (3-NBA) (Landvik et al. 2010). Individual chemical exposure investigated compounds in the absence (ActD, NQO, 3-NBA) or presence (CPP, NQO,

3-NBA) of metabolic activation. Binary and tertiary mixtures of ActD, NQO, and 3-NBA were tested in the absence of the metabolic system only. All conditions were also analyzed regarding effects on cell viability by means of a colorimetric method using the tetrazolium bromide salt (Mosmann 1983). This and similar methods are routinely applied in combination with diverse cell-based assays to evaluate chemicals and samples regarding cytotoxicity, with the minimum accepted cell viability being often set at 80% (Brinkmann et al. 2014; Xiao et al. 2016). Results are discussed considering different mechanisms of toxicity of chemicals and regarding the potential application of methods and the testing strategy for the evaluation of environmental contaminants and samples.

Materials and methods

Chemicals

The test chemicals (Table 1) ActD, CPP, and NQO were purchased from Sigma-Aldrich (Sigma-Aldrich Chemie GmbH, Steinheim, Germany) and 3-NBA from Chiron (Chiron AS, Trondheim, Norway). Stock and serial dilution solutions (following twofold serial dilutions based on log₁₀ M concentrations) were prepared by chemical dilution in dimethyl sulfoxide (DMSO, Sigma-Aldrich Chemie GmbH, Steinheim, Germany) and stored at 4 °C, except for the CPP solutions which were stored at –20 °C.

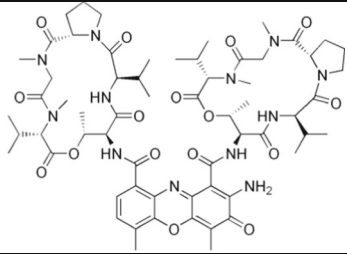
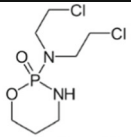
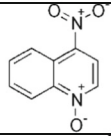
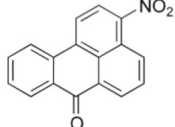
Cell culture

The human osteoblastic osteosarcoma cell line (U2OS) stably transfected with a luciferase-based p53 reporter construct was obtained from BioDetection Systems BV (BDS, Amsterdam, The Netherlands) and cultured as previously described (van der Linden et al. 2014). Briefly, cell cultures were maintained in a 1:1 mixture of Dulbecco's modified Eagle's medium and Ham's F12 medium (DMEM/F12) (Invitrogen Life Technologies, Darmstadt, Germany) with phenol red supplemented with 7.5% fetal calf serum (FCS) (Th. Geyer GmbH, Renningen, Germany), 0.2% penicillin/streptomycin solution (Invitrogen), 1% non-essential amino acids (Invitrogen), and G418 antibiotic (0.20 mg/ml) for the selective survival of transfected cells only. Cultures were maintained in a humidified atmosphere with 5% CO₂ at 37 °C until reaching around 90% confluence, when cells were used for tests or sub-cultures. Cells were passaged twice a week, and medium change was performed every 2 to 3 days.

p53 induction assessment

Cell cultures were trypsinized; cells were counted and resuspended in assay medium (phenol red-free 1:1 mixture of

Table 1 Test chemicals and respective CAS numbers, formulas, and molecular weights

Test chemicals	CAS number	Formula	Molecular weight (g/mol)	Structure
Actinomycin D (ActD)	50-76-0	C ₆₂ H ₈₆ N ₁₂ O ₁₆	1255.42	
Cyclophosphamide (CPP)	50-18-0	C ₇ H ₁₅ Cl ₂ N ₂ O ₂ P · H ₂ O	279.10	
4-Nitroquinoline 1-oxide (4-NQO)	56-57-5	C ₉ H ₆ N ₂ O ₃	190.16	
3-Nitrobenzanthrone (3-NBA)	17117-34-9	C ₁₇ H ₉ NO ₃	275.30	

DMEM/F12 supplemented with 5% of charcoal-stripped FCS, 0.2% penicillin/streptomycin solution, and 1% non-essential amino acids) to a final concentration of 10⁵ cells/ml. The cell suspension was transferred to 96-well plates (100 µl or 10⁴ cells per well), except the outermost wells, which were filled with 200 µl of phosphate-buffered saline (PBS, Sigma-Aldrich Chemie GmbH, Steinheim, Germany). After 16 to 20 h, the medium was refreshed and cells were incubated for 24 h with serial dilutions of the test chemicals (200 µl/well) at 37 °C and 5% CO₂. When cells were co-exposed with post-mitochondrial supernatant fraction from rat liver homogenate obtained by centrifugation at 9000×g (S9), each well received also 20 µl of freshly prepared S9 mix (10% S9, 200 µM NADPH, 3 mM glucose-6-phosphate, 0.3 U/ml glucose-6-phosphate dehydrogenase, and 5 mM magnesium chloride in assay medium). After 3 h, the medium was removed and cells were washed with PBS and received fresh assay medium (200 µl/well) for another 21 h until a total of 24-h incubation. Each plate contained also solvent controls (1% DMSO). All conditions were performed in triplicate wells in each test and contained final DMSO concentration of 1%. After the incubation period, the medium was removed and cells were lysed in 1% Triton X-100 lysis buffer (BDS). D-Luciferin solution (BDS illuminate mix) was added, and the luciferase activity was measured using a luminometer (GloMax® 96 Microplate Luminometer, Promega GmbH, Germany).

Cell viability assessment

Cell viability of individual chemicals and mixtures was evaluated through a colorimetric microplate assay with 3-(4,5-dimethylthiazol-2-yl)-2,5-diphenyltetrazolium bromide, which is reduced to formazan by viable cells (MTT test) (Mosmann 1983; Berridge et al. 2005). Briefly, cells were exposed following the same procedures as for p53 induction analysis. At the end of the 24-h incubation period and visual verification of no contamination evidence, medium was removed and each well received 100 µl of freshly prepared 0.5 mg/ml MTT in non-supplemented DMEM/F12 medium. In each plate, six wells containing no cells received the MTT solution for the measurement of the background signal. After 30 min of incubation at 37 °C and 5% CO₂, the occurrence of formazan crystals was confirmed by microscope observation. The medium was discharged; 200 µl of DMSO was added per well, and plates were shaken for 15 min for crystal solubilization. The amount of formed formazan was determined using a microplate spectrophotometer (Tecan Infinite® M200, Tecan, Switzerland) at an absorbance wavelength of 492 nm.

Exposure to individual substances and mixtures

Incubation in the presence of S9 mix was applied to evaluate NQO, 3-NBA, and the standard chemical CPP following individual chemical exposures. Incubation in the absence of S9 mix

was applied to evaluate NQO, 3-NBA, and the standard chemical ActD following individual exposures and also binary (ActD/3-NBA, NQO/3-NBA, ActD/NQO) and a tertiary mixture (ActD/NQO/3-NBA). Individual chemical and mixture exposure ranges (Table 2) evaluated chemicals following twofold serial dilutions were based on log10 M concentrations. For individual chemical exposure, highest test concentrations of ActD and CPP were adopted from the protocol provided by BDS, aiming to cover from none up to peak induction; for NQO ±S9, they were selected with respect to preliminary genotoxicity and cytotoxicity tests, and for 3-NBA, the highest test concentration was based on its solubility in aqueous solutions (PubChem) and according to previous studies. For the mixtures, ActD and NQO were evaluated following the same dilution series as for the individual chemical exposure, except that the respective highest concentrations were excluded. This procedure aimed to avoid the occurrence of reduced cell viability in the test of mixtures. The exposure concentration of 3-NBA was kept the same in all dilution steps in mixtures, being also the second highest concentration of the individual chemical exposure testing. For the test of individual chemicals, the p53 induction and MTT test experiments were repeated, respectively, 14 and 4 times for ActD, 7 and 3 times for CPP, 3 and 4 times for NQO –S9, 3 and 3 times for NQO +S9, 3 and 3 times for 3-NBA –S9, and 2 and 3 times for 3-NBA +S9. For the test of mixtures, the p53 induction and MTT test experiments were repeated three times.

Data analysis

The p53 induction results were expressed as induction factor (IF) values, obtained by normalizing the response of each concentration to the DMSO response. IF threshold values for occurrence of p53 induction activity were set at 1.7 and 2.0 for incubations in the absence and presence of S9 mix, respectively (van der Linden et al. 2014). The lowest concentration reaching the threshold value was identified as the lowest observed effect concentration (LOEC), and the concentration causing the highest IF value was described as the peak concentration. For cell viability, results were expressed as fold changes of measurements obtained from treated cells in comparison to cells exposed to DMSO only, after subtraction of

the average background signal from all conditions. Fold changes were then converted to cell viability percentage (%) values, considering the solvent control to present 100%. Cell viability inhibition concentration IC₅₀ and IC₂₀ values were obtained through three-parameter non-linear regression (bottom constrained to 0) using GraphPad Prism version 6 (GraphPad Software, San Diego, CA, USA). In order to evaluate the correlation between p53 induction and cellular viability, ratios between MTT IC₅₀ or IC₂₀ values and p53 LOEC or peak values were also calculated. The biological effects of the mixtures were estimated considering independent action and effect additivity. The predicted mixture responses were calculated as the sum of the respective individual chemical biological responses in the MTT and p53 assays as $E_{ABC}(c_A, c_B, c_C) = EA(c_A) + EB(c_B) + EC(c_C)$, with $E_{ABC}(c_A, c_B, c_C)$ being the predicted biological effects (E) following the exposure to a mixture containing the chemicals A, B, and C in the concentrations (c) $c_A, c_B,$ and $c_C,$ respectively, and $E_x(c_x)$ being the measured biological effects obtained for the respective single chemical exposures (Groten et al. 2001; SCHER, SCCS, SCENIHR 2012). The predicted mixture results were then compared to respective measured values obtained in the tests of mixtures.

Results and discussion

Individual chemical exposures

Considering results for the different compounds, profiles of cell viability IC₅₀ (M) values (Table 2: ActD –S9 < NQO +S9 < NQO –S9 < 3-NBA ±S9 < CPP –S9) tended to present direct correlation with p53 induction LOECs (M) (Table 3: ActD –S9 < NQO –S9 < NQO +S9 < 3-NBA ±S9 < CPP +S9), as can be observed in Fig. 1. The ratios between MTT IC₅₀ or IC₂₀ and p53 LOEC or peak are presented in Fig. 2.

Actinomycin D –S9

ActD –S9 gave the highest values of p53 induction factor among all chemicals (Table 4), with an IF peak of

Table 2 Exposure concentrations of individual chemicals and mixtures for bioassays performed in the presence (+S9) or absence (–S9) of metabolic activation systems

Test chemicals	Bioassays +S9	Bioassays –S9	
	Individual chemical (M)	Individual chemical (M)	Binary and tertiary mixtures (M)
ActD		$1 \times 10^{-6} - 1 \times 10^{-10}$	$1 \times 10^{-7} - 3 \times 10^{-11}$
NQO	$1 \times 10^{-4} - 1 \times 10^{-8}$	$1 \times 10^{-9} - 1 \times 10^{-5}$	$3 \times 10^{-6} - 3 \times 10^{-10}$
3-NBA	$9 \times 10^{-5} - 1 \times 10^{-8}$	$9 \times 10^{-5} - 1 \times 10^{-8}$	Constant at 3×10^{-5}
CPP	$1 \times 10^{-3} - 1 \times 10^{-7}$		

Table 3 Cell viability inhibition IC_{50} and IC_{20} (M) values plus respective 95% confidence intervals (CI) obtained in the MTT test following individual chemical exposures in the absence (–S9) and presence (+S9) of metabolic activation

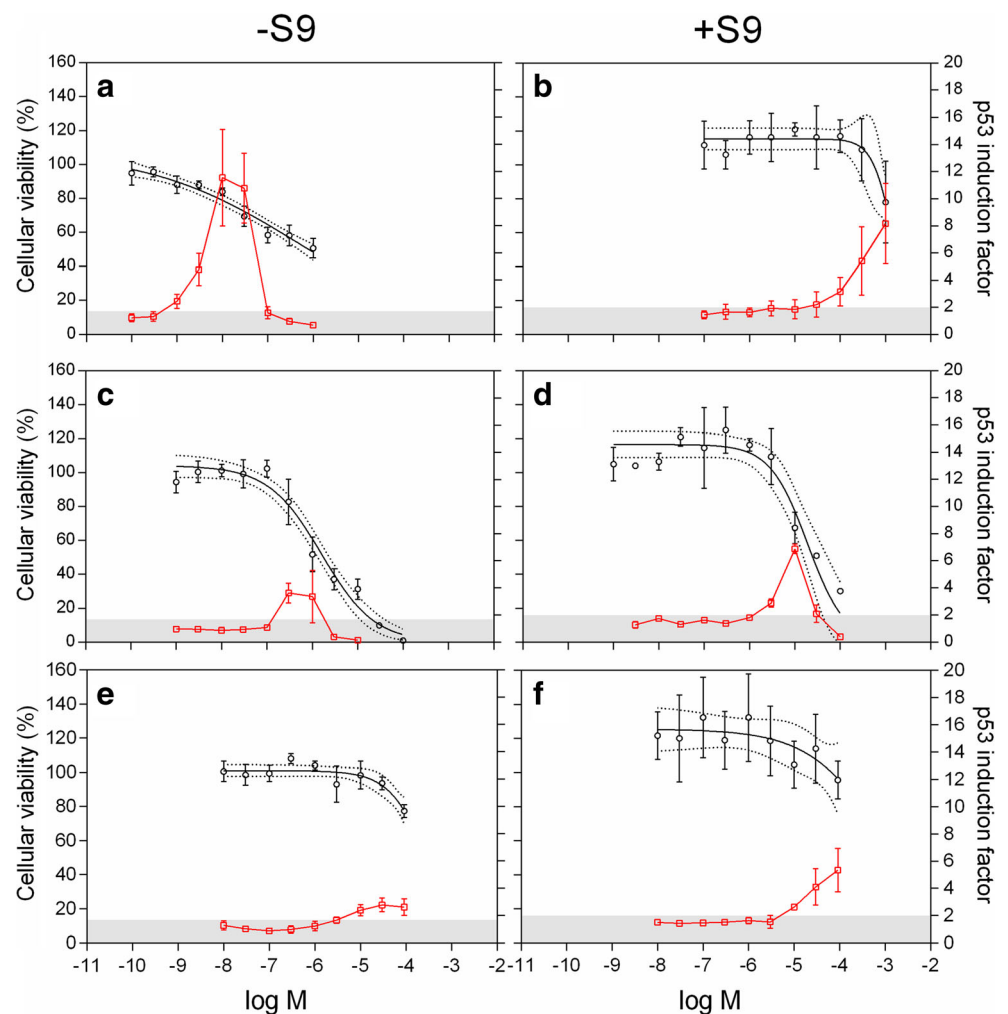
	Cell viability IC_{50} (M)		Cell viability IC_{20} (M)	
	IC_{50} and 95% CI		IC_{20} and 95% CI	
MTT –S9				
ActD	4.6×10^{-7}	1.6×10^{-7} to 1.3×10^{-6}	2.4×10^{-9}	1.2×10^{-10} to 4.8×10^{-8}
NQO	1.6×10^{-6}	1.1×10^{-6} to 2.3×10^{-6}	2.5×10^{-7}	1.2×10^{-7} to 5.0×10^{-7}
3-NBA	n.a.		7.6×10^{-5}	5.0×10^{-5} to 1.2×10^{-4}
MTT +S9				
CPP	n.a.		6.3×10^{-4}	3.0×10^{-4} to 1.3×10^{-3}
NQO	1.9×10^{-5}	1.1×10^{-5} to 3.2×10^{-5}	5.1×10^{-6}	2.4×10^{-6} to 1.1×10^{-5}
3-NBA	n.a.		7.3×10^{-5}	7.6×10^{-6} to 7.1×10^{-4}

n.a. not available

11.5 ± 3.6 . p53 induction LOEC (1 nM) and peak concentration (10 nM) were the same as those found in the method pre-validation study (van der Linden et al. 2014), and both

occurred at cell viabilities above 80% (Table 3, Fig. 1a). For ActD 30 nM, the high IF was maintained, but viability was slightly reduced ($70 \pm 7\%$), followed by further viability

Fig. 1 Cell viability (%; left y-axis) and p53 induction factor (right y-axis) of cells exposed in the absence (–S9) or presence (+S9) of S9 mix plotted versus the respective concentrations (log M, x-axis) of ActD (a), CPP (b), NQO (c, d), and 3-NBA (e, f). Shown are average values and standard errors for cell viability (black, circles) or p53 induction factors (red, squares), plus 95% confidence bands for viability. The shadowed areas indicate the threshold values for p53 induction activity in –S9 (1.7) and +S9 (2.0) tests. Number of MTT and p53 induction experiments, respectively: ActD (4, 14), CPP (3, 7), NQO –S9 (4, 3) and +S9 (3, 3), 3-NBA –S9 (3, 3) and +S9 (3, 2)



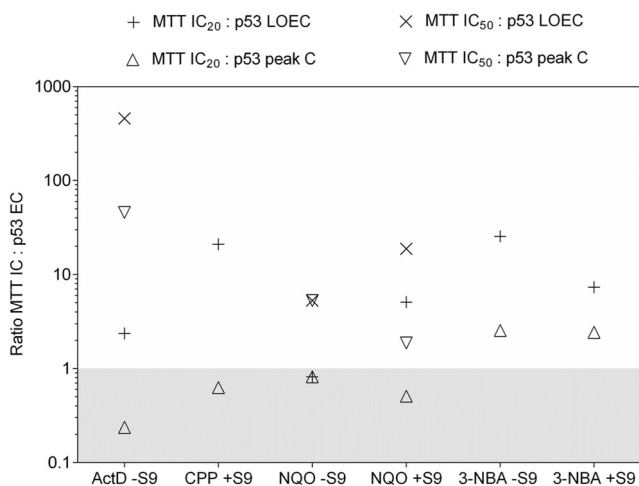


Fig. 2 Ratios between MTT cell viability inhibition IC_{50} and IC_{20} values and respective p53 effect concentration (EC), i.e., LOEC or peak concentration (peak C) for the different individual chemical exposures (*x*-axis). The *shadowed area* highlights ratio values equal to or lower than 1, indicating p53 effect concentration values that occurred at concentrations equal or higher than respective cell viability inhibition IC value

reduction and p53 IF drop below the threshold value (Fig. 1a) at concentrations ≥ 100 nM. Ratios of MTT to p53 effect concentrations were always higher than 1 except for $MTT_{IC_{20}}$ /

$p53_{peak}$ (around 0.25), which indicates that the concentration causing peak of p53 induction was circa four times higher than the cell viability inhibition IC_{20} .

ActD is an antineoplastic compound often applied for the treatment of tumors. Similar direct p53 induction and cytotoxicity profiles were described for experiments with diverse cell types, with 1 to 30 nM ActD causing increased p53 activity, expression, and phosphorylation, followed by decrease at 100 nM (Choong et al. 2009; Chen et al. 2014). While at the cytostatic low nanomolar range, ActD was described to cause ribosomal stress that leads to a decrease in MDM2 levels and consequently p53 stabilization and activation; at higher cytotoxic concentrations, the compound acts as a transcription blocker (Chen et al. 2014). Although the molecular mechanisms are not yet fully understood, it is already known that ActD inhibits RNA synthesis by binding to guanine residues and inhibiting DNA-dependent RNA polymerase (Choong et al. 2009) leading to the accumulation of free ribosomal proteins that can decrease the MDM2 function (van Leeuwen et al. 2011). Importantly, the compound was described to induce genotoxicity relevant endpoints such as the formation of histone gamma-H2AX foci (Mischo et al. 2005), which is a biomarker of DNA strand breaks and of micronucleus formation (Kuo and Yang 2008; Ivashkevich et al.

Table 4 LOEC and peak concentration (M) values for p53 induction factor for the individual compounds following exposure in the absence (-S9) or presence (+S9) of metabolic activation and for the mixtures in the absence of S9 mix

	LOEC (M)		Peak concentration (M)		Peak IF
	Average	Min/max	Average	Min/max	Average \pm SD
Individual chemicals -S9					
ActD	1×10^{-9}	$3 \times 10^{-10}/1 \times 10^{-9}$	1×10^{-8}	$1 \times 10^{-8}/3 \times 10^{-8}$	11.5 ± 3.6
NQO	3×10^{-7}	$3 \times 10^{-7}/3 \times 10^{-7}$	3×10^{-7}	$3 \times 10^{-7}/1 \times 10^{-6}$	3.6 ± 0.7
3-NBA	3×10^{-6}	$3 \times 10^{-6}/1 \times 10^{-5}$	3×10^{-5}	$3 \times 10^{-5}/1 \times 10^{-4}$	2.8 ± 0.5
Individual chemicals +S9					
CPP	3×10^{-5}	$3 \times 10^{-7}/1 \times 10^{-4}$	1×10^{-3}	$3 \times 10^{-4}/1 \times 10^{-3}$	8.2 ± 3
NQO	1×10^{-6}	$1 \times 10^{-8}/3 \times 10^{-6}$	1×10^{-5}	$1 \times 10^{-5}/1 \times 10^{-5}$	6.9 ± 0.9
3-NBA	1×10^{-5}	$1 \times 10^{-5}/1 \times 10^{-5}$	3×10^{-5}	$3 \times 10^{-5}/1 \times 10^{-4}$	4.1 ± 1.3
Binary mixtures -S9					
ActD/3-NBA					
ActD	3×10^{-11}	$3 \times 10^{-11}/3 \times 10^{-11}$	1×10^{-8}	$1 \times 10^{-8}/1 \times 10^{-8}$	11.1 ± 0.6
NQO/3-NBA					
NQO	3×10^{-10}	$3 \times 10^{-10}/1 \times 10^{-8}$	3×10^{-7}	$1 \times 10^{-7}/3 \times 10^{-7}$	4.8 ± 0.9
ActD/NQO					
ActD	1×10^{-9}	$1 \times 10^{-9}/1 \times 10^{-9}$	1×10^{-8}	$1 \times 10^{-8}/1 \times 10^{-8}$	7.7 ± 1.4
NQO	1×10^{-8}	$1 \times 10^{-8}/1 \times 10^{-8}$	1×10^{-7}	$1 \times 10^{-7}/1 \times 10^{-7}$	
Tertiary mixture -S9					
ActD/NQO/3-NBA					
ActD	3×10^{-11}	$3 \times 10^{-11}/3 \times 10^{-11}$	1×10^{-8}	$1 \times 10^{-8}/1 \times 10^{-8}$	8.6 ± 2.8
NQO	3×10^{-10}	$3 \times 10^{-10}/3 \times 10^{-10}$	1×10^{-7}	$1 \times 10^{-7}/1 \times 10^{-7}$	

Obtained LOEC average, minimum and maximum values, and IF averages and standard deviations are provided

2012). Therefore, the strong p53 induction identified in our study presents correlation with DNA damage markers.

Cyclophosphamide +S9

CPP +S9 caused the highest values of p53 induction factor for +S9 exposures (Table 4), with an IF peak of 8.2 ± 3.0 . The determined CPP p53 induction LOEC ($0.3 \mu\text{M}$) was lower than the obtained in the pre-validation study (van der Linden et al. 2014), and the later in fact agreed with our peak concentration of 1 mM. This difference might be related to the higher variability recognized to occur in assays containing metabolic system (van der Linden et al. 2014). Cytotoxic effects were not so evident in the tested concentration range, being possible to calculate only the IC₂₀ value (63 mM). The ratio $\text{MTT}_{\text{IC}_{20}}/\text{p53}_{\text{peak}}$ was lower than 1 (around 0.6), with the p53 peak occurring at a CPP concentration circa 1.6 times the cell viability IC₂₀.

CPP is a widely antineoplastic pharmaceutical often investigated in vitro and in vivo studies using rodents. Treatment of primary human cytotoxic T cells with circa $10 \mu\text{M}$ of a CPP-activated analog led to strong p53 induction, which was correlated with induced ROS production and nuclear relocation of mitochondrial apoptogenic factors (Strauss et al. 2007). In this way, the present results support the capability of the p53 assay to identify p53 induction intermediated by different molecular mechanisms. CPP also induced cardiotoxicity and increased mRNA expression of the p53 gene in rats (Asiri 2010), indicating potential organism-level relevance of our results. Due to its use as pharmaceutical, CPP contamination of aquatic environments can be of concern. While advanced treatment with ozonation can achieve its complete removal (Ferre-Aracil et al. 2016), conventional wastewater treatment achieves only partial reduction, with CPP concentrations up to 0.06 nM occurring in effluents (Steger-Hartmann et al. 1997). Furthermore, the DNA-damaging potential of CPP metabolites and transformation products might present a risk to aquatic environments since these compounds can occur in hospital wastewater (Česen et al. 2016).

4-Nitroquinoline 1-oxide ±S9

NQO caused intermediate values of p53 induction factors for exposures both with and without S9 mix (Table 4). For NQO –S9, the p53 LOEC and peak occurred at the same concentration ($0.3 \mu\text{M}$), being very close to the cell viability inhibition IC₂₀ ($0.25 \mu\text{M}$) and circa five times lower than the IC₅₀ ($1.6 \mu\text{M}$). Following metabolic activation, there was an increase in the p53 LOEC ($1 \mu\text{M}$) and peak concentrations ($10 \mu\text{M}$), and cell viability inhibition IC₂₀ ($5.1 \mu\text{M}$) and IC₅₀ ($19 \mu\text{M}$) were circa one order of magnitude higher. Still, the IF peak in +S9 (6.9) was nearly the double of the one in –S9 (3.6), which can be attributed to higher p53 induction by the metabolites when compared to the parent compound (Brüschhafer et al. 2016). In both –S9 and +S9

exposures, the ratio $\text{MTT}_{\text{IC}_{20}}/\text{p53}_{\text{peak}}$ was lower than 1 (around 0.6), indicating that the p53 peak was caused by concentrations higher than the respective cell viability IC₂₀. Therefore, for NQO, the assay ±S9 was able to adequately identify p53 induction despite of concurrent cytotoxic effects.

NQO is a compound often applied in positive control conditions of methods investigating genotoxicity. In previous studies, NQO –S9 caused circa 50% of cell viability at $1\text{--}2 \mu\text{M}$ after 24-h exposure to epidermoid carcinoma cells, which presented increased p53 expression already after 2 h of treatment (Han et al. 2007). In addition to cytotoxicity, NQO –S9 caused micronucleus formation in human lymphoblastoid cells, which was more evident in p53 dysfunctional lines (Brüschhafer et al. 2016). In vivo studies following treatment of rats with the NQO metabolite 4-hydroxyaminoquinoline 1-oxide identified that p53 expression, apoptosis, and cell proliferation occurred sequentially in pancreas, processes which are considered to be closely related with the compound carcinogenesis following DNA adduct formation (Imazawa et al. 2003). Again, the measured p53 induction can be correlated with other genotoxicity endpoints and demonstrates relevance to support in vivo investigations.

3-Nitrobenzanthrone ±S9

3-NBA caused the lowest values of p53 induction factor for exposures both with and without S9 mix (Table 4). For 3-NBA –S9, the p53 LOEC ($3 \mu\text{M}$) and peak ($30 \mu\text{M}$) were 25 and 2.5 times lower than the cell viability inhibition IC₂₀ ($76 \mu\text{M}$). Following metabolic activation, there was an increase in the LOEC ($10 \mu\text{M}$), but the peak ($30 \mu\text{M}$) and cell viability inhibition IC₂₀ ($73 \mu\text{M}$) were maintained. Such profile could indicate that the sensitivity of the assay was affected by the co-incubation with the metabolic activation system. Still, the IF peak in the +S9 experiments (4.1) was around 1.5 times higher than the one in –S9 (2.8), indicating that the assay +S9 is able to identify relevant p53 induction. Additionally, similarly to NQO, this profile can be attributed to higher p53 induction by 3-NBA metabolites when compared to the parent compound (IARC 2014). Cytotoxic effects were not so evident in the tested concentration range, being possible to calculate only the IC₂₀ value in both ±S9 (Table 3). Differently than for the other chemicals, the ratios between MTT and p53 effect concentration values were always higher than 1. Therefore, for 3-NBA ±S9, the peak and LOEC were achieved at concentrations lower than the cell viability inhibition IC₂₀. That indicates that for 3-NBA, the p53 induction activity would be identified even if exposure concentrations were limited to those occurring with minimum 80% of cell viability.

3-NBA is a diesel exhaust component considered as possibly carcinogenic to humans by the International Agency for Research on Cancer (IARC 2014). It causes DNA adduct formation and oxidative stress both in vitro and in vivo

(Nagy et al. 2007), and DNA strand breaks identified through the comet assay (Arlt et al. 2004). In experiments with human bronchial epithelial cells, 3-NBA in the low micromolar range caused increased p53 phosphorylation and nuclear translocation, formation of the DNA strand break marker gamma-H2AX, and apoptosis (Øya et al. 2011). However, our results are contrasting with an investigation on the effects of 3-NBA and its metabolite 3-aminobenzanthrone on mouse hepatoma cells, which described that although both compounds increased p53 phosphorylation, its translocation to the nucleus occurred only after 3-NBA exposure (Landvik et al. 2010). Such differences can be related to cell sensitivity variations or to the formation of other active 3-NBA metabolites in our study. 3-NBA results also support the relevance of the p53 assay to identify induction intermediated by diverse mechanisms and its correlation with diverse genotoxicity endpoints.

Binary and tertiary mixtures' p53 induction and cell viability

Predicted responses in the binary and tertiary mixtures, estimated by the sum of the respective measured individual chemical responses in the MTT and p53 assay, were compared to the measured values obtained in the tests of mixtures. In general, there was good agreement between predicted and

measured IF values for the lowest concentration ranges, while higher chemical concentrations caused instead lower than expected IF values (Figs. 3 and 4). For the four lower concentrations of the binary mixtures, the predicted and measured values were very similar, confirming additivity (Fig. 3b, c) or indicating slight synergism (Fig. 3a) for p53 induction. For the tertiary mixtures, instead there was infra-additivity tendency (Fig. 3d). As an outcome, predicted LOECs were always in agreement with measured values (Fig. 3). That suggests sensitivity of the assay to identify the activity even when mixtures of components are present. IF peaks instead tended to occur at concentrations lower than predicted, except for ActD/3-NBA for which it was maintained (Fig. 3a). Further, IF values for the peak and higher test concentrations tended to be lower than respective predicted values (Figs. 3 and 4), particularly for the binary ActD/NQO (Fig. 3c) and the tertiary (Fig. 3d) mixture. Such results indicate that the evaluation of mixtures might require careful selection of investigated concentration range in order to properly identify the peak of induction and estimate the respective magnitude of response.

Additivity of the p53 induction response is already explored for therapeutic use of pharmaceuticals. For ActD, combined drug administration applies low doses of the drug aiming to achieve increased p53 activation while avoiding undesired cytotoxic or DNA-damaging effects (Rao et al.

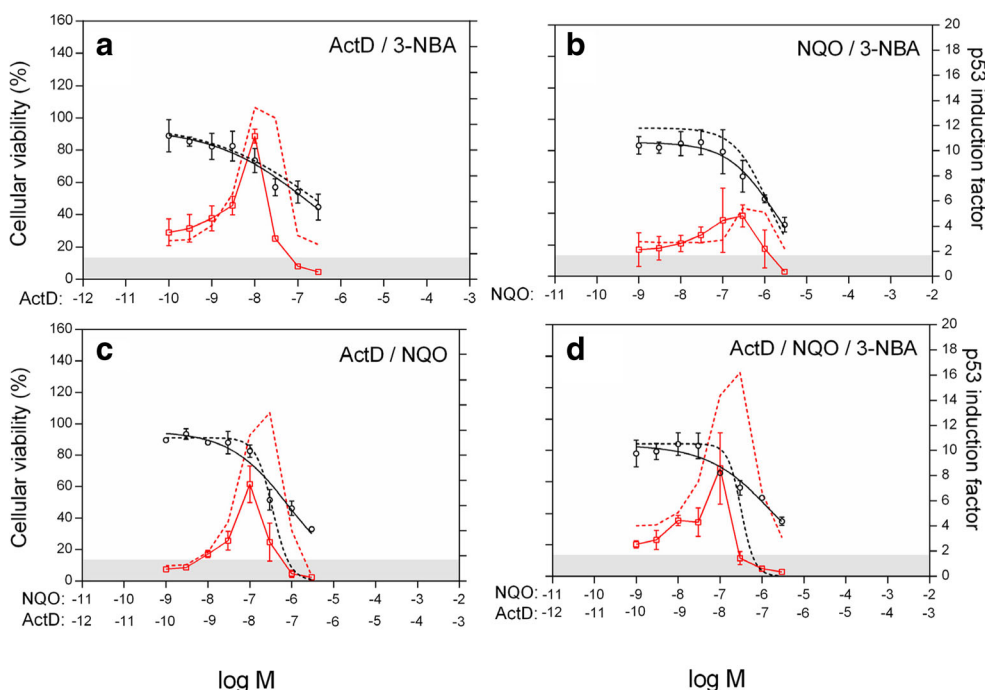


Fig. 3 Measured (full lines) and additivity-predicted (dotted lines) values of cellular viability (black, as % in left y-axis) and p53 induction factor (red, in right y-axis) plotted versus concentrations (log M) of the binary mixtures ActD/3-NBA (a), NQO/3-NBA (b), and ActD/NQO (c) and of the tertiary mixture ActD/NQO/3-NBA (d). The mixtures containing 3-NBA had 3×10^{-5} M of the chemical in all exposure conditions. Average

values (viability (black circles), induction factor (red squares)) and standard deviations are shown. The shaded areas indicate threshold values for p53 induction activity of 1.7. For all mixtures, three independent experiments were performed for the MTT assay and for the p53 induction test, respectively

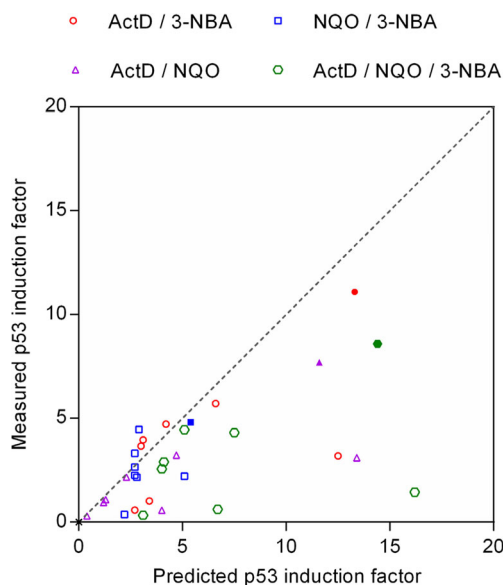


Fig. 4 Measured (*y*-axis) versus predicted (*x*-axis) p53 induction factor values for the binary and tertiary mixtures. Binary mixtures (ActD/3-NBA (*red circles*), NQO/3-NBA (*blue squares*), ActD/NQO (*purple triangles*)) presented similar predicted and measured p53 induction factor values at lower concentrations, while higher concentrations gave lower than expected values. The tertiary mixture (ActD/NQO/3-NBA (*green hexagons*)) presented prevalence of lower than expected values. The measured peaks of induction factor (indicated by respective *filled symbols*) were in general lower than respective predicted values

2010; Chen et al. 2014). Synergism has also been described for ActD in the low nanomolar range combined with antitumorigenic drugs (Choong et al. 2009). Similarly, our results indicate that at low concentration, additivity or even synergism occurred, while higher concentrations presented reduced p53 IF when compared to predicted values. That is in agreement with lower cell viability values obtained for the mixtures (Fig. 3) when compared to respective individual compounds (Fig. 1). Surprisingly, cell viability reduction at highest test concentrations was not as intensive as predicted for the binary mixture containing ActD/NQO (Fig. 3c) and for the tertiary (Fig. 3d) mixtures. Still, viability values reached circa 40% at highest test concentrations for both mixtures. Although p53 is discussed to present a protective role against DNA damage-induced cell death (Garner and Raj 2008), other factors might have interfered with exposures at higher concentrations such as chemical interactions between tested compounds.

Our study indicates that, resembling the therapeutic use of pharmaceuticals, additivity of p53 response is obtained when cells are exposed to mixtures of compounds presenting different mechanisms of toxicity. Such outcome supports the application of the p53 assay to investigate environmentally relevant mixtures or environmental samples. Similarly to chemical exposures, p53 peaks can occur at concentrations that cause cell viability below the 80% value (Fig. 3). Therefore, when

evaluating individual chemicals, mixtures, or samples for the occurrence of p53 induction, it is recommended to include also rather cytotoxic concentrations in the evaluated test range, reaching up to 50% of reduction in cell viability. Concentrations that cause more than 50% of cell viability reduction should however be interpreted with caution since non-specific responses caused by general cell stress can also occur (van der Linden et al. 2014).

Conclusions

This study demonstrated the ability of the p53 assay to identify p53 induction through different mechanisms and both with and without metabolic activation system. Additionally, the assay was efficient in identifying additivity of the p53 response when evaluating chemical mixtures, confirming its ability to identify mixture activity and potentially also of complex environmental samples. For such future applications, it is of relevance to consider in experimental planning and evaluation that p53 peaks can be lower and occur at lower test concentrations than for respective individual chemicals. Further, cytotoxicity evaluation should be applied to support the selection of concentration ranges and also the interpretation of the p53 assay results. In this sense, our study demonstrates that the often-used minimum 80% cell viability threshold to set the maximum exposure concentration for cell-based bioassays is not optimal for the p53 assay. Future evaluations of mixtures or environmental samples through the p53 assay are recommended to include concentrations that cause up to 50% cell viability reduction in the evaluated test range. In this way, the identification of the LOEC and peak concentration will unlikely be missed for the compounds and mixture components that cause meaningful p53 induction concurrently with cytotoxic effects.

Acknowledgements Thanks to the RWTH colleague Simone Hotz for the support during the establishment of the cell line and assay in our laboratory. Thanks to BioDetection Systems BV (BDS, Amsterdam, The Netherlands) for supplying the cell line and respective culture and method protocols. Thanks to Promega GmbH, Germany, and to Tecan Group Ltd., Switzerland, for their contribution to this study as a partner of the Students Lab “Fascinating Environment” at Aachen Biology and Biotechnology (ABBt). This study was supported by the EDA-EMERGE ITN project within the EU Seventh Framework Program (FP7-PEOPLE-2011-ITN) under the grant agreement number 290100.

References

- Arlt VM, Cole KJ, Phillips DH (2004) Activation of 3-nitrobenzanthrone and its metabolites to DNA-damaging species in human B lymphoblastoid MCL-5 cells. *Mutagenesis* 19:149–156
- Asiri YA (2010) Probucol attenuates cyclophosphamide-induced oxidative apoptosis, p53 and Bax signal expression in rat cardiac tissues. *Oxidative Med Cell Longev* 3:308–316
- Beckerman R, Prives C (2010) Transcriptional regulation by p53. *Cold Spring Harb Perspect Biol* 2(8):a000935

- Bensaad K, Rouillard D, Soussi T (2001) Regulation of the cell cycle by p53 after DNA damage in an amphibian cell line. *Oncogene* 20: 3766–3775
- Berridge MV, Herst PM, Tan AS (2005) Tetrazolium dyes as tools in cell biology: new insights into their cellular reduction. *Biotechnol Annu Rev* 11:127–152
- Bhaskaran A, May D, Rand-Weaver M, Tyler CR (1999) Fish p53 as a possible biomarker for genotoxins in the aquatic environment. *Environ Mol Mutagen* 33:177–184
- Briat A, Vassaux G (2008) A new transgenic mouse line to image chemically induced p53 activation in vivo. *Cancer Sci* 99:683–688
- Brinkmann M, Blenkle H, Salowsky H, Bluhm K, Schiwiy S, Tiehm A et al (2014) Genotoxicity of heterocyclic PAHs in the micronucleus assay with the fish liver cell line RTL-W1. *PLoS One* 9:e85692
- Brüsehauer K, Manshian BB, Doherty AT, Zaïr ZM, Johnson GE, Doak SH et al (2016) The clastogenicity of 4NQO is cell-type dependent and linked to cytotoxicity, length of exposure and p53 proficiency. *Mutagenesis* 31:171–180
- Česen M, Kosjek T, Buseti F, Kompare B, Heath E (2016) Human metabolites and transformation products of cyclophosphamide and ifosfamide: analysis, occurrence and formation during abiotic treatments. *Environ Sci Pollut Res* 23:11209–11223
- Chen C-S, Ho D-R, Chen F-Y, Chen C-R, Ke Y-D, Su J-GJ (2014) AKT mediates actinomycin D-induced p53 expression. *Oncotarget* 5: 693–703
- Choong ML, Yang H, Lee MA, Lane DP (2009) Specific activation of the p53 pathway by low dose actinomycin D: a new route to p53 based cyclotherapy. *Cell Cycle* 8:2810–2818
- Clewell RA, Sun B, Adeleye Y, Carmichael P, Efremenko A, McMullen PD et al (2014) Profiling dose-dependent activation of p53-mediated signaling pathways by chemicals with distinct mechanisms of DNA damage. *Toxicol Sci* 142:56–73
- Duerksen-Hughes PJ, Yang J, Ozcan O (1999) p53 induction as a genotoxic test for twenty-five chemicals undergoing in vivo carcinogenicity testing. *Environ Health Perspect* 107:805–812
- Ferre-Aracil J, Valcárcel Y, Negreira N, de Alda ML, Barceló D, Cardona SC et al (2016) Ozonation of hospital raw wastewaters for cytostatic compounds removal. Kinetic modelling and economic assessment of the process. *Sci Total Environ* 556:70–79
- Garner E, Raj K (2008) Protective mechanisms of p53-p21-pRb proteins against DNA damage-induced cell death. *Cell Cycle* 7:277–282
- Groten JP, Feron VJ, Suhnel J (2001) Toxicology of simple and complex mixtures. *Trends Pharmacol Sci* 22:316–322
- Han H, Pan Q, Zhang B, Li J, Deng X, Lian Z et al (2007) 4-NQO induces apoptosis via p53-dependent mitochondrial signaling pathway. *Toxicology* 230:151–163
- Harris SL, Levine AJ (2005) The p53 pathway: positive and negative feedback loops. *Oncogene* 24:2899–2908
- IARC. IARC Working Group on the Evaluation of Carcinogenic Risk to Humans. Diesel and gasoline engine exhausts and some nitroarenes. Lyon (FR): International Agency for Research on Cancer (2014) (IARC Monographs on the Evaluation of Carcinogenic Risks to Humans, No. 105.) 3-NITROBENZANTHRONE. Available from: <http://www.ncbi.nlm.nih.gov/books/NBK294272/>. 2014
- Imazawa T, Nishikawa A, Toyoda K, Furukawa F, Mitsui M, Hirose M (2003) Sequential alteration of apoptosis, p53 expression, and cell proliferation in the rat pancreas treated with 4-hydroxyaminoquinoline 1-oxide. *Toxicol Pathol* 31:625–631
- Ivashkevich A, Redon CE, Nakamura AJ, Martin RF, Martin OA (2012) Use of the γ -H2AX assay to monitor DNA damage and repair in translational cancer research. *Cancer Lett* 327:123–133
- Jin L, Gaus C, Escher BI (2015) Adaptive stress response pathways induced by environmental mixtures of bioaccumulative chemicals in dugongs. *Environ Sci Technol* 49:6963–6973
- Kester HA, Sonneveld E, van der Saag PT, van der Burg B (2003) Prolonged progestin treatment induces the promoter of CDK inhibitor p21Cip1, Waf1 through activation of p53 in human breast and endometrial tumor cells. *Exp Cell Res* 284:262–271
- Knight AW, Little S, Houck K, Dix D, Judson R, Richard A et al (2009) Evaluation of high-throughput genotoxicity assays used in profiling the US EPA ToxCast chemicals. *Regul Toxicol Pharmacol* 55:188–199
- Kumari R, Kohli S, Das S (2014) p53 regulation upon genotoxic stress: intricacies and complexities. *Mol Cell Oncol* 1:e969653
- Kuo LJ, Yang LX (2008) Gamma-H2AX—a novel biomarker for DNA double-strand breaks. *In Vivo* 22:305–309
- Landvik NE, Arlt VM, Nagy E, Solhaug A, Tekpli X, Schmeiser HH et al (2010) 3-Nitrobenzanthrone and 3-aminobenzanthrone induce DNA damage and cell signalling in Hepal1c7 cells. *Mutat Res Fundam Mol Mech Mutagen* 684:11–23
- Lavin MF, Gueven N (2006) The complexity of p53 stabilization and activation. *Cell Death Differ* 13:941–950
- Lutzker SG, Mathew R, Taller DR (2001) A p53 dose-response relationship for sensitivity to DNA damage in isogenic teratocarcinoma cells. *Oncogene* 20:2982–2986
- Mischo HE, Hemmerich P, Grosse F, Zhang S (2005) Actinomycin D induces histone γ -H2AX foci and complex formation of γ -H2AX with Ku70 and nuclear DNA helicase II. *J Biol Chem* 280:9586–9594
- Mosmann T (1983) Rapid colorimetric assay for cellular growth and survival: application to proliferation and cytotoxicity assays. *J Immunol Methods* 65:55–63
- Nagy E, Adachi S, Takamura-Enya T, Zeisig M, Möller L (2007) DNA adduct formation and oxidative stress from the carcinogenic urban air pollutant 3-nitrobenzanthrone and its isomer 2-nitrobenzanthrone, in vitro and in vivo. *Mutagenesis* 22:135–145
- Øya E, Øvrevik J, Arlt VM, Nagy E, Phillips DH, Holme JA (2011) DNA damage and DNA damage response in human bronchial epithelial BEAS-2B cells following exposure to 2-nitrobenzanthrone and 3-nitrobenzanthrone: role in apoptosis. *Mutagenesis* 26(6):697–708
- Rao B, van Leeuwen IMM, Higgins M, Campbell J, Thompson AM, Lane DP et al (2010) Evaluation of an actinomycin D/VX-680 aurora kinase inhibitor combination in p53-based cyclotherapy. *Oncotarget* 1:639–650
- Rutkowski R, Hofmann K, Gartner A (2010) Phylogeny and function of the invertebrate p53 superfamily. *Cold Spring Harb Perspect Biol* 2: a001131
- Salazar AM, Ostrosky-Wegman P, Menendez D, Miranda E, Garcia-Carranca A, Rojas E (1997) Induction of p53 protein expression by sodium arsenite. *Mutat Res Fundam Mol Mech Mutagen* 381: 259–265
- Salazar AM, Sordo M, Ostrosky-Wegman P (2009) Relationship between micronuclei formation and p53 induction. *Mutat Res Genet Toxicol Environ Mutagen* 672:124–128
- SCHER, SCCS, SCENIHR (2012) Opinion on the toxicity and assessment of chemical mixtures. European Commission, Brussels
- Sohn TA, Bansal R, Su GH, Murphy KM, Kern SE (2002) High-throughput measurement of the Tp53 response to anticancer drugs and random compounds using a stably integrated Tp53-responsive luciferase reporter. *Carcinogenesis* 23:949–958
- Steger-Hartmann T, Kümmerer K, Hartmann A (1997) Biological degradation of cyclophosphamide and its occurrence in sewage water. *Ecotoxicol Environ Saf* 36:174–179
- Storer NY, Zon LI (2010) Zebrafish models of p53 functions. *Cold Spring Harb Perspect Biol* 2:a001123
- Strauss G, Westhoff MA, Fischer-Posovszky P, Fulda S, Schanbacher M, Eckhoff SM et al (2007) 4-Hydroperoxy-cyclophosphamide mediates caspase-independent T-cell apoptosis involving oxidative stress-induced nuclear relocation of mitochondrial apoptogenic factors AIF and EndoG. *Cell Death Differ* 15:332–343
- van der Linden SC, von Bergh ARM, van Vught-Lussenburg BMA, Jonker LRA, Teunis M, Krul CAM et al (2014) Development of a panel of high-throughput reporter-gene assays to detect genotoxicity

- and oxidative stress. *Mutat Res Genet Toxicol Environ Mutagen* 760:23–32
- van Leeuwen IM, Higgins M, Campbell J, Brown CJ, McCarthy AR, Pirrie L et al (2011) Mechanism-specific signatures for small-molecule p53 activators. *Cell Cycle* 10:1590–1598
- Wernersson A-S, Carere M, Maggi C, Tusil P, Soldan P, James A et al (2015) The European technical report on aquatic effect-based monitoring tools under the water framework directive. *Environ Sci Eur* 27:1–11
- Xiao H, Kuckelkorn J, Nüßler LK, Floehr T, Hennig MP, Roß-Nickoll M et al (2016) The metabolite 3,4,3',4'-tetrachloroazobenzene (TCAB) exerts a higher ecotoxicity than the parent compounds 3,4-dichloroaniline (3,4-DCA) and propanil. *Sci Total Environ* 551–552:304–316
- Yang J, Duerksen-Hughes P (1998) A new approach to identifying genotoxic carcinogens: p53 induction as an indicator of genotoxic damage. *Carcinogenesis* 19:1117–1125
- Yeh RYL, Farré MJ, Stalter D, Tang JYM, Molendijk J, Escher BI (2014) Bioanalytical and chemical evaluation of disinfection by-products in swimming pool water. *Water Res* 59:172–184
- Zajkowicz A, Gdowicz-Klosok A, Krzesniak M, Scieglinska D, Rusin M (2015) Actinomycin D and nutlin-3a synergistically promote phosphorylation of p53 on serine 46 in cancer cell lines of different origin. *Cell Signal* 27:1677–1687